International Journal of Environmental Sciences
ISSN: 2229-7359
Vol. 11 No. 8, 2025
https://theaspd.com/index.php

Invisible Threats: Mobile Phone Radiation And Its Influence On Gliclazide Stability

Jay Ahire[*1], Mukesh Mohite[2], Sarita Sasane[3]
[1,2,3]Department of Pharmaceutical Quality Assurance, Dr. D.Y. Patil College of Pharmacy, Akurdi Pune 44

Abstract

Introduction: *Non-ionizing electromagnetic radiation (EMR) from mobile devices has been suggested to influence the stability of pharmaceuticals. This study investigates the effect of Bluetooth (active RF emission) and Flight mode (minimal RF emission) exposure on the structural and thermal stability of Gliclazide using Fourier Transform Infrared Spectroscopy (FTIR) and Differential Scanning Calorimetry (DSC), alongside in vivo hypoglycaemic evaluation in diabetic Wistar rats.*

Materials and Methods: *Gliclazide tablets were exposed to EMR for 6, 12, and 18 hours under controlled conditions. Structural alterations were assessed by FTIR (4000–400 cm^{-1}, ATR mode), and thermal behaviour by DSC (25–300°C, 10°C/min heating rate, N_2 atmosphere). The in vivo study involved alloxan-induced diabetic Wistar rats treated with control or EMR-exposed Gliclazide (5 mg/kg), with fasting blood glucose measured on days 0, 7, and 14.*

Results: *FTIR revealed progressive alterations in characteristic functional group peaks with increasing Bluetooth exposure duration, particularly in –NH stretching and sulfonyl group vibrations, indicating molecular modifications. DSC thermograms of Bluetooth-exposed samples showed reduced melting endotherm and enthalpy, suggesting decreased crystallinity, while Flight mode–exposed samples exhibited comparatively minor shifts. In vivo, Bluetooth-exposed Gliclazide demonstrated a significantly attenuated glucose-lowering effect compared to both Flight mode–exposed and control groups ($p<0.05$), with the greatest loss of efficacy after 18 h exposure.*

Conclusion: *Bluetooth EMR causes more pronounced structural and functional impairment of Gliclazide than Flight mode exposure, potentially reducing its therapeutic efficacy. These findings underscore the need for EMR-conscious storage and handling guidelines for sensitive drugs.*

Keywords: *Gliclazide; Electromagnetic radiation; Bluetooth; Flight mode; FTIR; Differential Scanning Calorimetry (DSC)*

INTRODUCTION

Diabetes mellitus is a chronic metabolic disorder characterized by persistent hyperglycaemia resulting from impaired insulin secretion, insulin action, or both. It poses a significant global health challenge, with the International Diabetes Federation estimating that over 530 million adults were affected in 2021—a number projected to surpass 640 million by 2030. Beyond its metabolic implications, diabetes is associated with severe microvascular and macrovascular complications, including retinopathy, nephropathy, neuropathy, cardiovascular disease, and stroke, contributing substantially to morbidity, mortality, and economic burden worldwide.

The management of diabetes often involves pharmacological interventions aimed at achieving optimal glycaemic control. Gliclazide, a second-generation sulfonylurea, is widely prescribed for type 2 diabetes mellitus due to its glucose-lowering efficacy and relatively favourable safety profile. However, the stability and therapeutic effectiveness of oral hypoglycaemic agents can be influenced by environmental factors during storage, transport, and use. Among these, electromagnetic fields (EMFs)—emanating from modern telecommunication devices—have emerged as a potential but understudied variable.

EMFs are generated by both natural and artificial sources, spanning a broad frequency spectrum from extremely low frequency (ELF) to radiofrequency (RF) and microwave ranges. Mobile phones, Wi-Fi routers, Bluetooth devices, and other wireless technologies operate primarily in the RF range (10 MHz– 300 GHz). While regulatory guidelines by bodies such as the International Commission on Non- Ionizing Radiation Protection (ICNIRP) are designed to prevent harmful thermal effects, growing evidence suggests that prolonged, low-intensity, non-ionizing EMF exposure may induce subtle biological changes through non-thermal mechanisms, such as oxidative stress and altered molecular interactions.

In daily life, pharmaceutical products may be inadvertently exposed to EMFs during storage near mobile phones, wearable devices, or wireless charging stations. Such exposure could potentially alter physicochemical properties, impacting drug overall bioavailability. Despite the ubiquity of EMFs in modern environments, systematic studies investigating their impact on drug stability remain limited.

This study focuses on evaluating the influence of mobile phone-generated EMFs—specifically Bluetooth mode (active RF emission) and Flight mode (minimal RF emission)—on the structural and functional integrity of Gliclazide. Using a combination of analytical techniques, including Fourier Transform Infrared Spectroscopy

(FTIR), Differential Scanning Calorimetry (DSC), the research aims to provide novel insights into how non-ionizing radiation may affect pharmaceutical stability. Understanding these interactions is crucial for ensuring drug efficacy, patient safety, and the development of updated guidelines for medication handling in an increasingly wireless world.[1-15]

MATERIALS AND METHODS

Gliclazide 80 mg tablets (standard formulation) were obtained from a local pharmacy. A Xiaomi Redmi Note 10 Pro smartphone served as the EMR source. Two exposure modes were studied: **Bluetooth mode** and **Flight mode**. Tablets were placed at a fixed distance from the device maintained at 25°C (±2°C) and 60% (±5%) relative humidity. Exposure durations were 6, 12, or 18 hours. Control tablets were kept in identical environmental conditions but shielded from EMF.

Analytical procedures were as follows:

FTIR Spectroscopy: Tablet samples (n=3 per condition) were finely powdered and analysed by ATR- FTIR (PerkinElmer Spectrum Two). Spectra (4000–400 cm^–1) were collected (4 cm^–1 resolution, 32 scans). Characteristic bond vibrations (e.g. O–H, N–H, C=O, C–N, S=O) were compared between exposed and control samples to detect structural alterations. [16-22]

Differential Scanning Calorimetry (DSC): 5–10 mg of each sample was sealed in aluminium pans and heated from 30°C to 300°C at 10°C/min under nitrogen (Shimadzu DSC-60). Melting onset, peak temperatures, and fusion enthalpy (ΔH) were recorded for each tablet. Loss of crystallinity or polymorphic changes were inferred from shifts in thermal parameters. [23-28]

Animal Study: Diabetes was induced in overnight-fasted Wistar rats by intraperitoneal injection of alloxan (120-150 mg/kg in citrate buffer, pH 4.5). Animals with fasting glucose ≥250 mg/dL after 72 hrs were included. Rats were divided into nine groups: control Gliclazide, Bluetooth-exposed Gliclazide (6, 12, 18 h), Flight mode–exposed Gliclazide (6, 12, 18 h), and diabetic untreated controls. Gliclazide was administered orally (5mg/kg). Blood glucose was measured on days 0, 7, and 14 via tail vein sampling using a glucometer. [28-34]

RESULT:

Table 1: FTIR Spectroscopy Analysis

FTIR spectrum of non-exposed Gliclazide showing characteristic functional group peaks	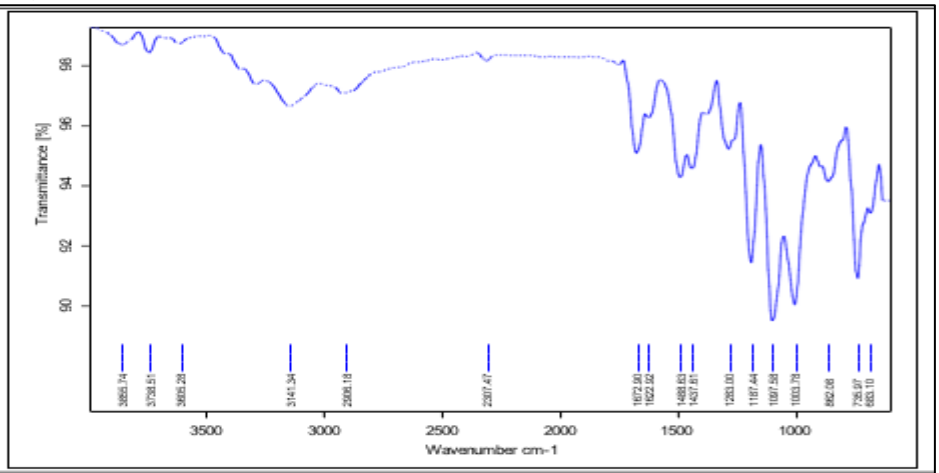
FTIR spectrum of Gliclazide after 6h Bluetooth exposure revealing initial vibrational changes	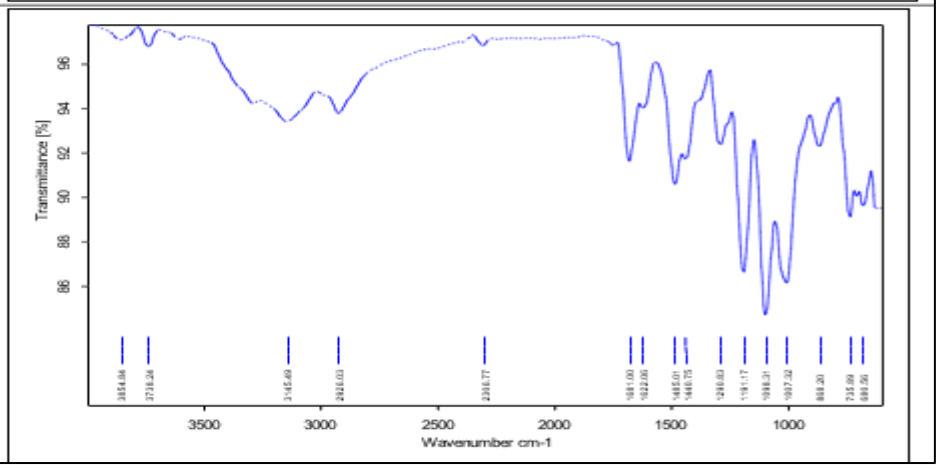

FTIR spectrum of Gliclazide after 12h Bluetooth exposure demonstrating progressive alteration in molecular bonding	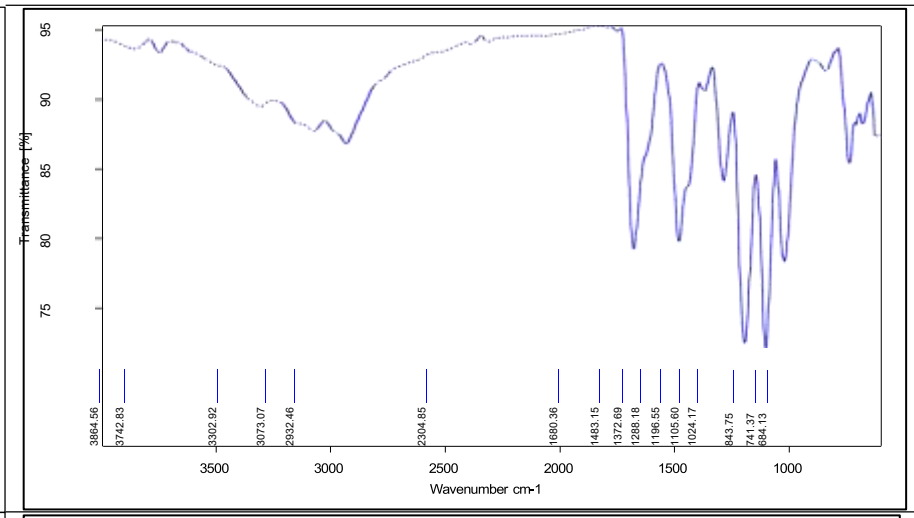
FTIR spectrum of Gliclazide after 18h Bluetooth exposure showing substantial modifications in functional group signatures	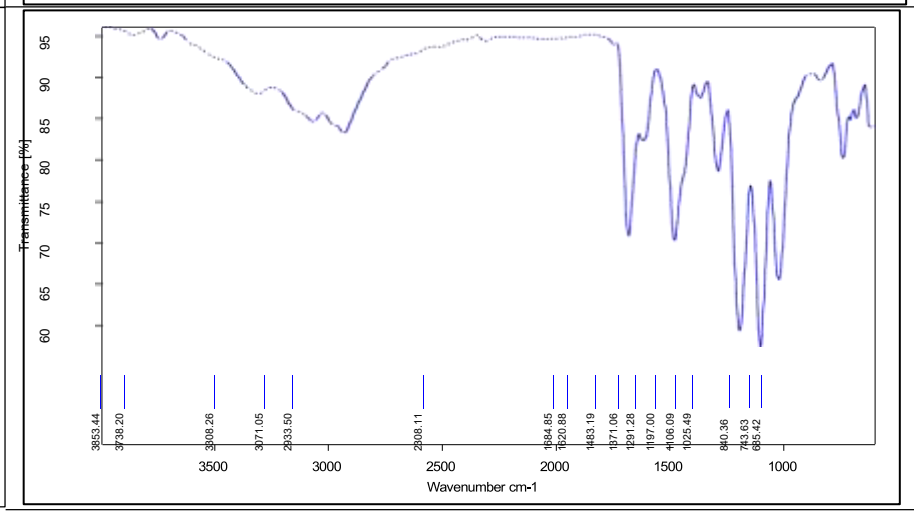

Table 2: Characteristic FTIR peaks of Gliclazide following Bluetooth exposure.

Functional Group	Non-exposed (cm^{-1})	6h Exposed (cm^{-1})	12h Exposed (cm^{-1})	18h Exposed (cm^{-1})	Interpretation
O-H stretching (free)	3855.74	3854.84	3864.56	3864.56	Slight increase in wavenumber after prolonged exposure indicates weakening of hydrogen bonding
N-H stretching (free)	3783.51	3738.24	3742.83	3742.83	Significant decrease suggesting altered amine environment
O-H stretching (bonded)	3605.28	Not observed	Not observed	Not observed	Complete disappearance indicates disruption of hydrogen bonding network
N-H stretching (bonded)	3141.34	3145.49	3302.92	3302.92	Substantial shift to higher wavenumber reveals modification in amid eenvironment
C-H stretching (aromatic)	Not observed	Not observed	3073.07	3073.07	New peak formation indicating altered aromatic ring environment
C-H stretching (aliphatic)	2806.18	2925.03	2932.46	2932.46	Significant shift suggests conformational changes in aliphatic chains
S=O stretching	2307.47	2308.77	2304.85	2304.85	Minor changes indicating relative stability of sulfonyl group

C=O stretching (amide)	1672.90	1681.00	1680.36	1680.36	Shift to higher wavenumber suggests decreased hydrogen bonding at carbonyl oxygen
C=N stretching	1628.52	1622.09	Not observed	Not observed	Disappearance after 12h exposure indicates significant structural modification
C=C stretching (aromatic)	1489.83	1485.91	1483.15	1483.15	Progressive decrease suggesting reduced aromaticity
CH_2 bending	1437.61	1440.75	1372.98	1372.98	Substantial shift indicates altered methylene environment
C-N stretching	1283.00	1290.83	1289.18	1289.18	Slight increase suggests modified electron distribution around
S=O asymmetric stretching	1187.44	1181.17	1196.85	1196.85	Fluctuating values indicate changing sulfonamide environment
S=O symmetric stretching	1109.78	1109.31	1105.56	1105.56	Minor decrease suggesting slight alteration in sulfonyl group
C-O stretching	1003.96	1007.32	1024.17	1024.17	Significant increase indicates modified oxygen-containing moiety
C-H out-of-plane bending	882.06	886.20	843.75	843.75	Substantial shift suggests altered aromatic substitution pattern
C-S stretching	795.97	795.99	741.37	741.37	Major decrease after 12h exposure indicates modified sulfur-carbon bond
Ring deformation	683.10	683.69	684.13	684.13	Minimal change suggests relative stability of core ring structure

Table 3:FTIR Spectroscopy Analysis(Flight mode)

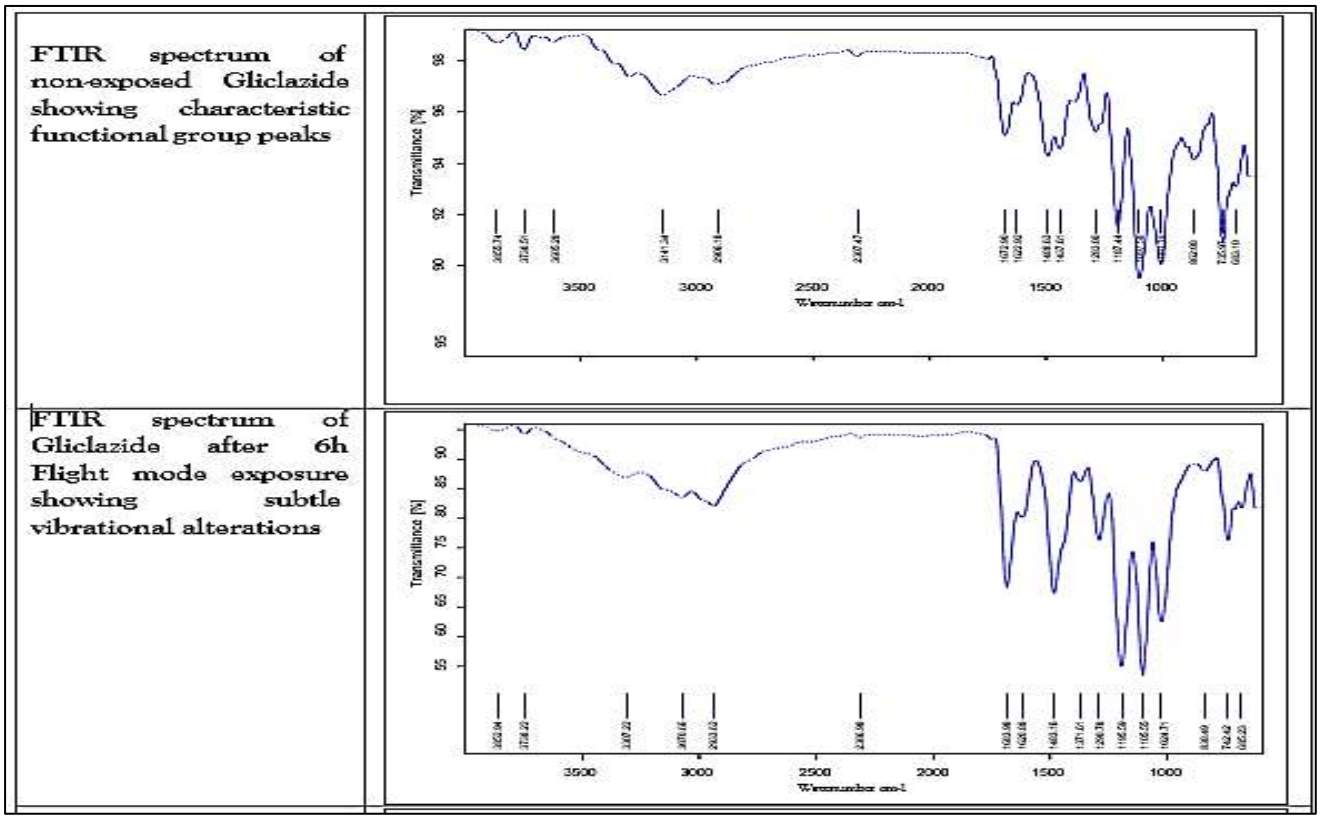

FTIR spectrum of Gliclazide after 12h Flight mode exposure revealing moderate changes in functional group signatures	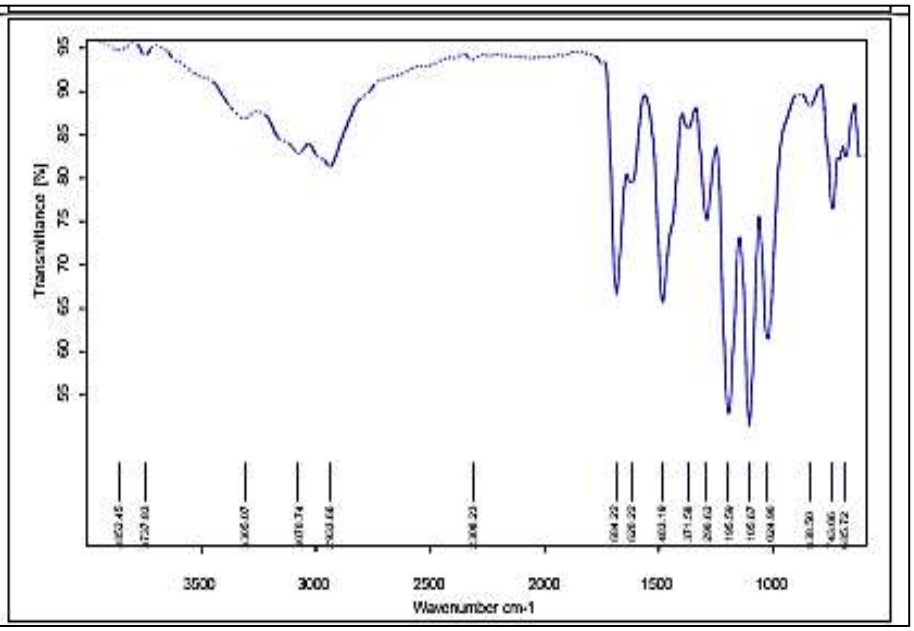

FTIR SPECTRUM OF

Gliclazide after 18h Flight mode exposure demonstrating significant molecular bonding modifications	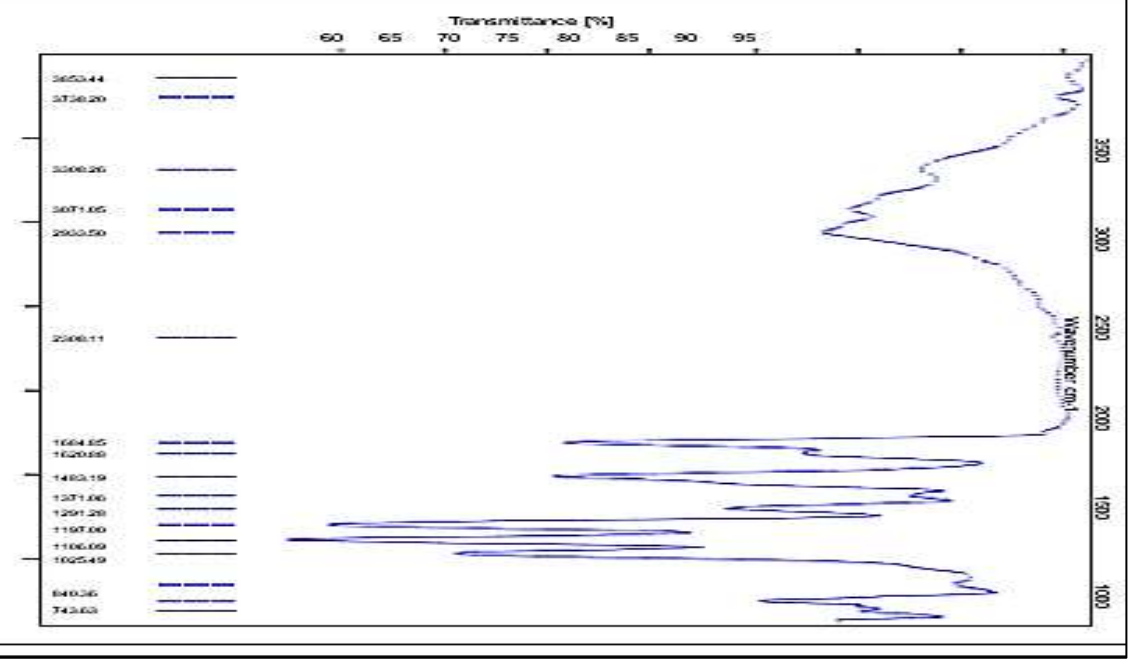

Table 4: Characteristic FTIR peaks of Gliclazide following Flight mode exposure.

Functional Group	Non-exposed (cm^{-1})	6h Exposed (cm^{-1})	12h Exposed (cm^{-1})	18h Exposed (cm^{-1})	Interpretation
O-H stretching (free)	3855.74	3852.94	3852.45	3853.44	Slight decrease followed by minimal recovery suggesting rearrangement of hydroxyl interactions
N-H stretching (free)	3783.51	3738.22	3737.83	3738.20	Significant decrease (45 cm^{-1}) stabilizing after initial exposure indicating permanent alteration in amine environment
O-H stretching (bonded)	3605.28	Not observed	Not observed	Not observed	Complete disappearance indicating disruption of hydrogen bonding network
N-H stretching (bonded)	3141.34	Not observed	Not observed	Not observed	Complete disappearance of original peak
New N-H stretching	Not observed	3307.22	3305.07	3308.26	Formation of new N-H environment with different hydrogen bonding characteristics
C-H stretching (aromatic)	Not observed	3070.66	3070.74	3071.05	New peak formation indicating modified aromatic ring environment
C-H stretching (aliphatic)	2806.18	2933.92	2933.66	2933.50	Substantial shift (+127 cm^{-1}) suggesting significant conformational changes in aliphatic chains
S=O stretching	2307.47	2306.98	2308.23	2308.11	Minimal fluctuations indicating relative stability of sulfonyl group
C=O stretching (amide)	1672.90	1683.98	1684.22	1684.85	Progressive increase (+12 cm^{-1}) suggesting decreased hydrogen bonding at carbonyl oxygen
C=N stretching	1628.52	1620.98	1620.22	1620.88	Significant decrease (-7.6 cm^{-1}) indicating weakened C=N bond
C=C stretching (aromatic)	1489.83	1483.16	1483.19	1483.19	Consistent decrease suggesting modified aromaticity
CH_2 bending	1437.61	1371.61	1371.58	1371.08	Substantial decrease (-66.5 cm^{-1}) indicating major change in methylene environment
C-N stretching	1283.00	Not observed	Not observed	1291.28	Initial disappearance followed by reappearance at higher wavenumber

					suggesting reorganization of C-N bonds
S=O asymmetric stretching	1187.44	1207.98	1207.96	1197.00	Increase followed by partial recovery indicating electronic redistribution around sulfonamide
N-C=O stretching	Not observed	1159.58	1159.57	Not observed	Transient formation of new vibration mode that disappears after extended exposure
S=O symmetric stretching	1109.78	1105.55	1105.67	1105.49	Slight decrease suggesting minor alteration in sulfonyl group
C-O stretching	1003.96	1024.71	1024.90	1025.49	Progressive increase (+21.5 cm^{-1}) indicating significant modification of oxygen- containing moiety
C-H out-of-plane	882.06	898.49	838.50	840.36	Fluctuating values suggesting dynamic changes in aromatic substitution pattern
C-S stretching	795.97	742.22	743.09	776.33	Substantial decrease followed by partial recovery indicating reversible modification of C-S bond
Ring deformation	683.10	683.33	683.92	685.42	Progressive slight increase suggesting gradual alteration of core ring structure

Table 5: DSC Thermal Analysis(Bluetooth)

DSC thermogram of non-Exposed Gliclazide showing characteristic melting endotherm	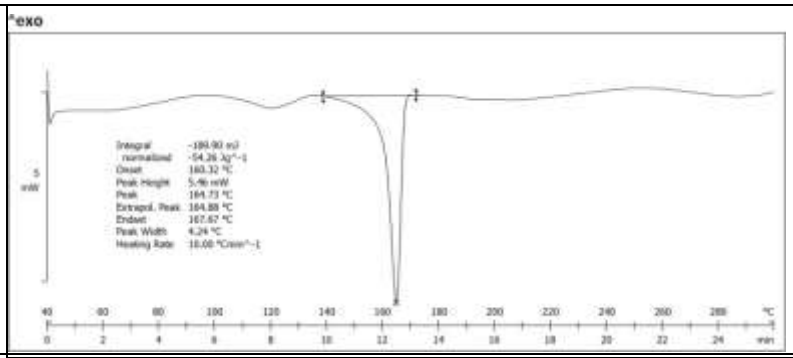
DSC thermogram of Gliclazide after 6h Bluetooth exposuredemonstrating significant modification in thermal properties	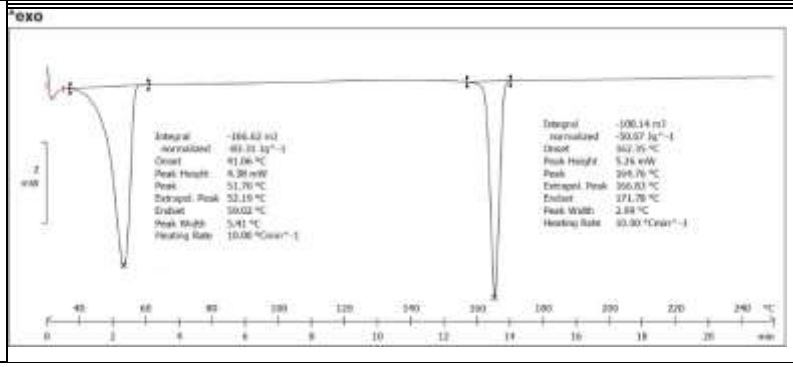

DSC thermogram of Gliclazide after 12h Bluetooth exposure demonstrating significant modification in thermal properties	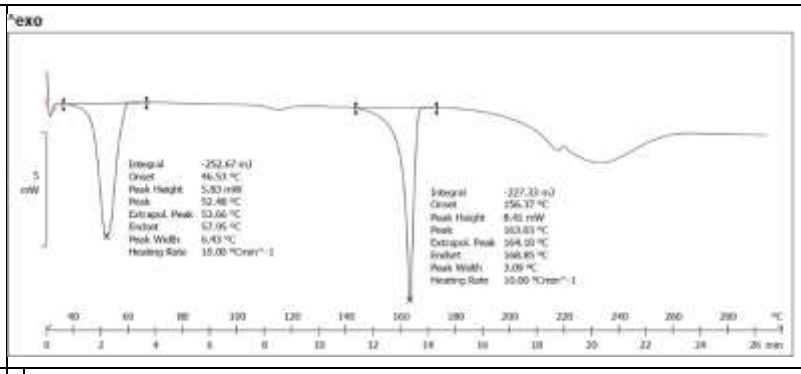
DSC thermogram of Gliclazide after 18h Bluetooth exposure demonstrating significant modification in thermal properties	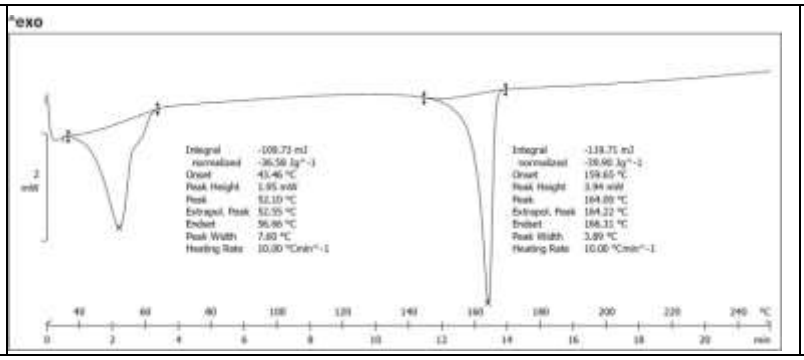

Table 6: DSC thermal parameters of Gliclazide following Bluetooth exposure.

Exposure Condition	Onset Temp (°C)	Peak Temp (°C)	Endset Temp (°C)	Peak Height (mW)	Enthalpy ΔH (mJ)	Normalized Enthalpy (J/g)	Peak Width (°C)
Non-exposed Control	160.32	164.73	167.67	5.46	-189.90	-54.26	4.24
6h Bluetooth	162.35	164.76	171.78	5.26	-100.14	-50.07	2.99
12h Bluetooth	156.37	163.03	168.85	8.41	-227.33	-	3.09
18h Bluetooth	159.65	164.00	166.31	3.94	-119.71	-39.90	3.89

Interpretation: Progressive reduction in enthalpy and altered peak shapes imply diminished crystalline order with Bluetooth exposure. This aligns with FTIR evidence of hydrogen-bond collapse and structural degradation.

Table 7: DSC Thermal Analysis (Flight mode)

DSC thermogram of non-Exposed Gliclazide showing characteristic melting endotherm	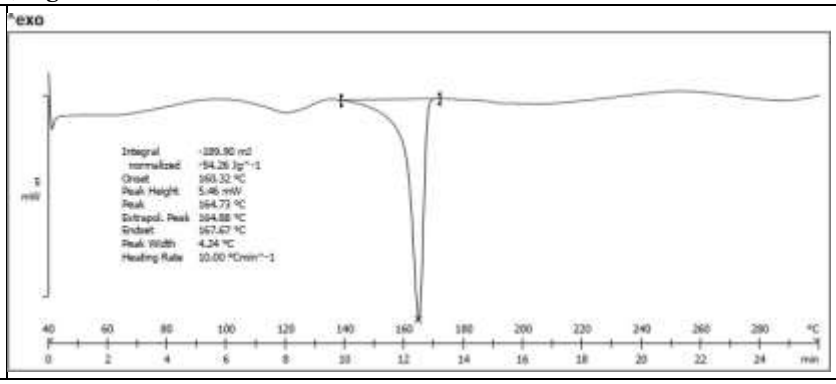

DSC thermogram of Gliclazide after 6h Flight mode exposure revealing altered thermal properties	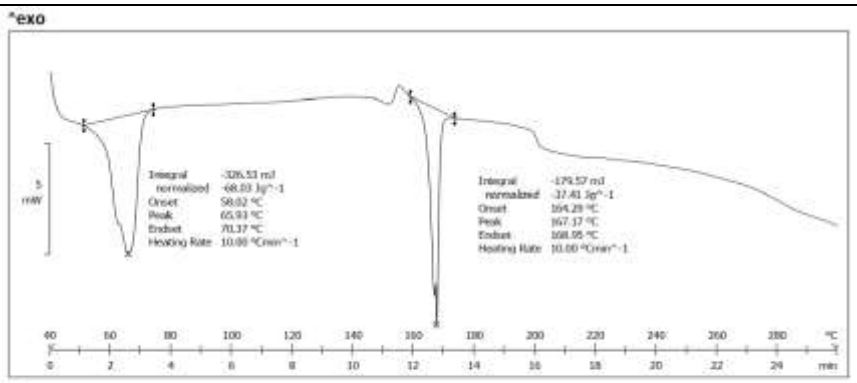
DSC thermogram of Gliclazide after 12h Flight mode exposure revealing altered thermal properties	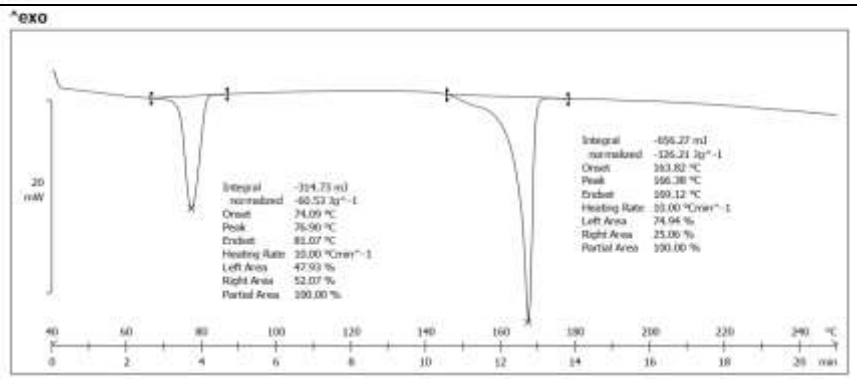
DSC thermogram of Gliclazide after 18h Flight mode exposure revealing altered thermal properties	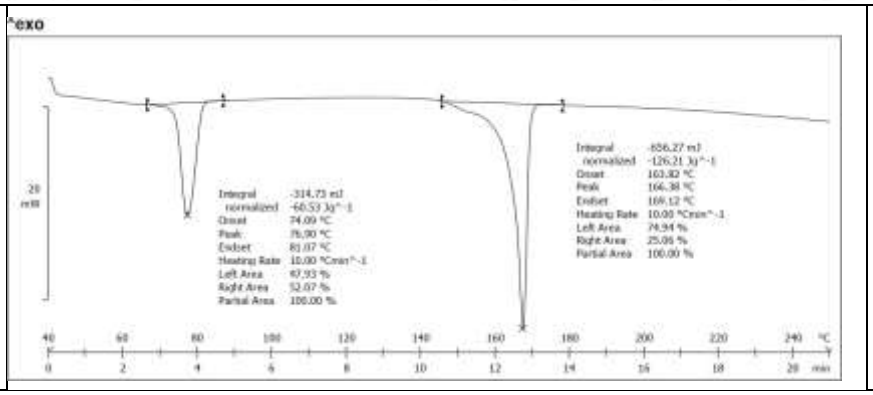

Table 8: Complete DSC Thermal Parameters Analysis - Flight Mode Exposure

Exposure Condition	Onset Temp (°C)	Peak Temp (°C)	Endset Temp (°C)	Peak Height (mW)	Enthalpy ΔH (mJ)	Normalized Enthalpy (J/g)	Peak Width (°C)
Non-exposed Control	160.32	64.73	167.67	5.46	-189.90	54.26	4.24
6h Flight Mode	58.02	65.93	70.37	-	-336.53	-68.03	-
	164.29	167.17	168.95	-	-179.57	-37.41	-
12h Flight Mode	74.09	76.90	81.07	-	-314.73	-60.53	7.0
	163.82	166.38	169.12	-	-656.27	-126.21	-
18h Flight Mode	74.09	76.90	81.07	-	-314.73	-60.53	7.0
	163.82	166.38	169.12	-	-656.27	-126.21	-

Interpretation: The reproducible low-temperature events alongside slightly higher main melting peaks suggest reorganization or polymorphic adjustment, potentially toward more ordered states for certain domains. The larger-magnitude normalized enthalpy reported for main melting at 12–18h implies complex redistributions of crystalline and semi-crystalline fractions, consistent with annealing or recrystallization phenomena initiated by environmental conditioning.

ETHICAL APPROVAL: Animal study approved by IAEC [Approval No.:

(DYPCOP/IAEC/2025/16/32)] and conducted per CPCSEA guidelines. Housing, diet, and humane endpoints complied with institutional SOPs.

Table: 9: Animal Activity -Blood Glucose Level

Group	Rat 1	Rat 2	Rat 3	Rat 4	Rat 5	Rat 6	Average
Normal control	78	82	80	88	79	84	81.83
Induction control	284	286	290	301	294	298	292.17
Standard	239	243	236	248	235	241	240.33
Bluetooth 6h Day 0	243	235	247	239	244	238	241.0
Bluetooth 6h Day 7	238	232	243	234	240	233	236.67
Bluetooth 6h Day 14	235	229	240	231	239	232	234.33
Bluetooth 12h Day 0	252	258	249	254	248	259	253.33
Bluetooth 12h Day 7	250	254	252	251	249	257	252.17
Bluetooth 12h Day 14	248	252	250	249	247	254	250.0
Bluetooth 18h Day 0	268	259	265	270	261	264	264.5
Bluetooth 18h Day 7	269	262	264	268	258	266	264.5
Bluetooth 18h Day 14	267	260	262	265	257	264	262.5
Flight Mode 6h Day 0	248	244	251	239	253	238	245.5
Flight Mode 6h Day 7	246	242	249	240	251	243	245.17
Flight Mode 6h Day 14	244	240	247	238	249	241	243.17
Flight Mode 12h Day 0	254	249	255	250	247	244	249.83
Flight Mode 12h Day 7	251	247	253	248	246	242	247.83
Flight Mode 12h Day 14	249	245	251	246	243	240	245.67
Flight Mode 18h Day 0	268	254	267	264	255	269	262.83
Flight Mode 18h Day 7	265	251	264	261	252	266	259.83
Flight Mode 18h Day 14	262	248	261	258	249	263	256.83

Interpretation: The in vivo data demonstrate that Gliclazide retained antihyperglycemic activity across all exposure conditions, as evidenced by consistent reductions in fasting blood glucose (FBG) from baseline (Day0) to Day14 in all treated groups relative to the diabetic (induction) control. Normal controls remained normoglycemic, confirming expected physiological ranges, while the induction control maintained markedly elevated FBG, validating successful diabetic modelling and providing an appropriate disease benchmark.

Within the Bluetooth-exposed cohorts, a clear exposure-duration gradient emerged: the 6h group exhibited the largest numeric decline in FBG over 14 days, whereas 12h and 18h groups showed progressively smaller declines. This monotonic attenuation suggests that prolonged active RF exposure may subtly diminish the apparent antihyperglycemic effect of Gliclazide in vivo over the study window. Mechanistically, this pattern aligns with the physicochemical findings indicating greater structural disruption and reduced crystallinity with longer Bluetooth exposure, which could influence dissolution, bioavailability, or the proportion of intact active moiety reaching systemic circulation.

In contrast, the Flight mode cohorts showed modest but consistent improvements in FBG across all durations, with the 18h group achieving the largest numeric reduction among Flight mode conditions. This trend is congruent with solid-state and spectroscopic indicators of structural reorganization rather than degradation under Flight mode, including evidence suggestive of recrystallization or improved lattice order. Such changes can rationally lead to more predictable release characteristics and sustained pharmacodynamic effect without compromising molecular integrity.

DISCUSSION

EMR exposure altered Gliclazide's functional group environments (FTIR) and thermal behaviour (DSC), indicating changes in hydrogen bonding, conformational arrangement, and possibly polymorphic state. Such physicochemical modifications plausibly impair dissolution or interaction with biological targets, matching the observed reduction in antihyperglycemic efficacy in vivo. Bluetooth- mode, representing active radio transmission, consistently induced greater structural drift and functional loss than Flight mode, likely due to higher near-field EMR activity.

DSC low-temperature events under Flight mode suggest moisture uptake or formation of new phases, whereas Bluetooth runs showed pronounced enthalpy changes and variability in peak characteristics, potentially reflecting partial amorphization or polymorphic transitions. The disappearance/shift of bonded O–H/N–H and C=N signals supports disruption of intra-/intermolecular hydrogen networks relevant to the sulfonylurea structure.

Practical implication: Keeping EMR-sensitive medications away from actively transmitting devices may reduce stability risks. Packaging with EM shielding or clear storage guidance could mitigate degradation.

CONCLUSION

Bluetooth-mode EMR exposure from mobile phones caused significant structural, thermal, and functional degradation of Gliclazide, as shown by FTIR, DSC, and reduced antihyperglycemic efficacy in vivo. Flight mode exposure produced comparatively minor effects, with minimal loss of stability or activity. These findings suggest that prolonged proximity of EMR-sensitive drugs to active wireless devices may compromise therapeutic performance, warranting careful storage practices and further investigation across other pharmaceuticals.

ACKNOWLEDGMENTS

The authors thank the Department of Pharmaceutical Chemistry, [Dr. D.Y. Patil College of Pharmacy, Akurdi], for laboratory and animal facility support, and [individuals/units] for instrumentation access (FTIR/DSC).

SUMMARY

Prolonged Bluetooth EMF exposure reduced the structural stability and glucose-lowering efficacy of Gliclazide, while Flight mode caused minimal or protective effects. FTIR and DSC analyses confirmed greater molecular and thermal changes with Bluetooth exposure, correlating with reduced therapeutic performance

in diabetic rats.

REFERENCES

1. International Diabetes Federation. IDF Diabetes Atlas, 10th ed.; International Diabetes Federation: Brussels, 2021.
2. American Diabetes Association. 2. Classification and Diagnosis of Diabetes: Standards of Medical Care in Diabetes—2022. Diabetes Care 2022, 45 (Suppl 1), S17–S38.
3. American Diabetes Association. 6. Glycemic Targets: Standards of Medical Care in Diabetes— 2022. Diabetes Care 2022, 45 (Suppl 1), S83–S96.
4. Matthews, D. R.; Hosker, J. P.; Rudenski, A. S.; Naylor, B. A.; Treacher, D. F.; Turner, R. C. Homeostasis Model Assessment: Insulin Resistance and β-Cell Function from Fasting Plasma Glucose and Insulin Concentrations in Man. Diabetologia 1985, 28 (7), 412–419.
5. DeFronzo, R. A.; Ferrannini, E.; Groop, L.; Henry, R. R.; Herman, W. H.; Holst, J. J.; et al. Type 2 Diabetes Mellitus. Nat. Rev. Dis. Primers 2015, 1, 15019. [Verify exact article number/pagination as needed.]
6. Hirata, A.; Diao, Y.; Onishi, T.; Sasaki, K.; Ahn, S.; Colombi, D.; et al. Assessment of Human Exposure to Electromagnetic Fields: Review and Future Directions. IEEE Trans. Electromagn. Compat. 2021, 63 (5), 1619–1630.
7. International Commission on Non-Ionizing Radiation Protection. Guidelines for Limiting Exposure to Electromagnetic Fields (100 kHz to 300 GHz). Health Phys. 2020, 118 (5), 483–
524.
8. World Health Organization. WHO Handbook on Indoor Radon: A Public Health Perspective, 2nd ed.; World Health Organization: Geneva, 2014.
9. Schuermann, D.; Mevissen, M. Manmade Electromagnetic Fields and Oxidative Stress— Biological Effects and Consequences for Health. Int. J. Mol. Sci. 2021, 22 (7), 3772.
10. Bosch-Capblanch, X.; Esu, E.; Oringanje, C. M.; Dongus, S.; Jalilian, H.; Eyers, J.; et al. The Effects of Radiofrequency Electromagnetic Fields Exposure on Human Self-Reported Symptoms: A Systematic Review of Human Experimental Studies. Environ. Int. 2024, 187, 108612.
11. Foster, K. R.; Moulder, J. E. Wi-Fi and Health: Review of Current Status of Research. Health Phys. 2013, 105 (6), 561–575.
12. Hardell, L.; Carlberg, M. Health Risks from Radiofrequency Radiation, Including 5G, Should Be Assessed by Experts with No Conflicts of Interest. Oncol. Lett. 2019, 17 (5), 5097–5100.
13. National Academies of Sciences, Engineering, and Medicine. An Evaluation of the Department of Defense's Approach to Preventing Exposures to Harmful Levels of Radiofrequency Radiation; The National Academies Press: Washington, DC, 2020.
14. Levitt, B. B.; Lai, H. C.; Manville, A. M. Effects of Non-Ionizing Electromagnetic Fields on Flora and Fauna: Rising Ambient EMF Levels in the Environment. Rev. Environ. Health 2022, 37 (1), 81–122.
15. Frei, P.; Mohler, E.; Bürgi, A.; Fröhlich, J.; Neubauer, G.; Braun-Fahrländer, C.; et al. A Prediction Model for Personal Radio Frequency Electromagnetic Field Exposure. Sci. Total Environ. 2009, 408 (1), 102–108.
16. Smith, B. Infrared Spectral Interpretation: A Systematic Approach, 2nd ed.; CRC Press: Boca Raton, FL, 2011.
17. Stuart, B. Infrared Spectroscopy: Fundamentals and Applications; John Wiley & Sons: Chichester, UK, 2004.
18. Nandiyanto, A. B. D.; Ragadhita, R.; Fiandini, M. Interpretation of Fourier Transform Infrared Spectra (FTIR): A Practical Approach in the Polymer/Plastic Thermal Decomposition. Indones.
J. Sci. Technol. 2023, 8 (1), 113–126.
19. Coates, J. Interpretation of Infrared Spectra, a Practical Approach. In Encyclopedia of Analytical Chemistry; Meyers, R. A., Ed.; John Wiley & Sons: Chichester, UK, 2000; pp 10815–10837.
20. PerkinElmer. ATR-FTIR Spectroscopy: Fundamentals and Applications; Application Note; PerkinElmer: Waltham, MA, 2018.
21. Griffiths, P. R.; de Haseth, J. A. Fourier Transform Infrared Spectrometry, 2nd ed.; John Wiley & Sons: Hoboken, NJ, 2007.
22. Socrates, G. Infrared and Raman Characteristic Group Frequencies: Tables and Charts, 3rd ed.; John Wiley & Sons: Chichester, UK, 2001.
23. Höhne, G.; Hemminger, W.; Flammersheim, H.-J. Differential Scanning Calorimetry, 2nd ed.; Springer: Berlin, 2003.
24. Wunderlich, B. Thermal Analysis of Polymeric Materials; Springer: Berlin, 2005.
25. ASTM International. ASTM E1269-11(2018): Standard Test Method for Determining Specific Heat Capacity by Differential Scanning Calorimetry; ASTM International: West Conshohocken, PA, 2018.
26. Fatah, H.; Claverie, J.; Poncet, S. Thermal Characterization of Phase Change Materials by Differential Scanning Calorimetry: A Review. Appl. Sci. 2022, 12 (23), 12019.
27. Haines, P. J., Ed. Principles of Thermal Analysis and Calorimetry; Royal Society of Chemistry: Cambridge, UK, 2002.
28. Gill, P.; Moghadam, T. T.; Ranjbar, B. Differential Scanning Calorimetry Techniques: Applications in Biology and Nanoscience. J. Biomol. Tech. 2010, 21 (4), 167–193.
29. Srinivasan, K.; Viswanad, B.; Asrat, L.; Kaul, C. L.; Ramarao, P. Combination of High-Fat Diet-Fed and Low-Dose Streptozotocin-Treated Rat: A Model for Type 2 Diabetes and Pharmacological Screening. Pharmacol. Res. 2005, 52 (4), 313–320.
30. Szkudelski, T. The Mechanism of Alloxan and Streptozotocin Action in β-Cells of the Rat Pancreas. Physiol. Res. 2001, 50 (6), 537–546.
31. Rakieten, N.; Rakieten, M. L.; Nadkarni, M. V. Studies on the Diabetogenic Action of Streptozotocin. Cancer Chemother. Rep. 1963, 29, 91–98.
32. National Research Council. Guide for the Care and Use of Laboratory Animals, 8th ed.; The National Academies Press:

Washington, DC, 2011.

33. CCSEA (formerly CPCSEA). Guidelines for Laboratory Animal Facility; Committee for the Control and Supervision of Experiments on Animals: New Delhi, India, 2018.

34. Morton, D. B.; Griffiths, P. H. Guidelines on the Recognition of Pain, Distress and Discomfort in Experimental Animals and an Hypothesis for Assessment. Vet. Rec. 1985, 116 (16), 431– 436.

35. Mohite, M. T.; Sharma, P.; Sharma, J.; Chaudhari, P.; Kore, S. Impact of Mobile Radiations on Gliclazide Tablet Formulation. Int. J. Pharm. Investigation 2023, 13 (3), 471–475.

36. More, A.; Topale, S.; Mohite, M.; Ahire, J. Mobile Radiation and Medications: A Comprehensive Review of Potential Interactions and Implications. Tanz J. [Year, volume, issue, page range to be verified]; [Confirm final bibliographic details].